

Retrieval of wheat bio-physical attributes from hyperspectral data and SAILH+PROSPECT radiative transfer model

Clement Atzberger^a, Thomas Jarmer^a, Martin Schlerf^a, Benjamin Kötzel^b and Willy Werner^c

^a University of Trier, Remote Sensing Department, Behringstrasse, D-54286 Trier, Germany, atzberger@feut.de

^b University of Zurich, Remote Sensing Laboratories, Switzerland

^c University of Trier, Department of Geobotany, Germany

ABSTRACT

A simple soil reflectance parameterization was empirically calibrated and integrated into the SAILH+PROSPECT canopy reflectance model to assess simultaneously LAI and canopy chlorophyll content from hyperspectral reflectance data. Model inversion was performed using an artificial neural net (ANN) trained on synthetic reflectance spectra that were generated by the extended canopy reflectance model. For validation, a completely independent data set was used consisting of field reflectance measurements and corresponding LAI and chlorophyll data. Results obtained on the validation data set were very promising. The coefficient of determination (R^2) varied between 0.86 and 0.87 (LAI and canopy chlorophyll content, respectively) and the root mean squared error (RMSE) between 0.83 (LAI; $m^2 m^{-2}$) and 0.66 (canopy chlorophyll content; $g m^{-2}$). The trained ANN was also applied to an airborne HyMAP image to demonstrate the applicability of the inversion approach to remote sensing data. The retrieved canopy chlorophyll contents and soil brightness values showed a reasonable correlation to on-site final yield measurements acquired two months after the image data acquisition.

Keywords: winter wheat, reflectance model, SAILH, PROSPECT, soil reflectance parameterization, leaf area index, canopy chlorophyll content, artificial neural net, HyMAP, hyperspectral reflectance

1 INTRODUCTION

The retrieval of bio-physical canopy variables by means of remote sensing is an important prerequisite for site-specific agriculture [1], [2]. This importance stems from the fact, that variables such as leaf area index (LAI) or chlorophyll content indicate the actual status of the crop and also its (potential) productivity. Crop growth can be derived, for example, from LAI through mechanistic growth models [3], [4], [5].

Bio-physical variables can either be mapped by means of empirical-statistical methods [6], [7], or by means of physically based approaches (i.e. the inversion of radiative transfer models) [8], [4]. Generally, the radiative transfer based approach is preferred, since it allows more physical insight into the system behavior [9], [10], [11]. Moreover, radiative transfer models can in principle be more easily transferred to different measurement conditions and crop types and are particularly well suited for hyperspectral and multi-directional data sets. Empirical-statistical methods have the advantages that they are simple and easy to use. They may also serve as benchmark models against which radiative transfer models can be compared [12].

For the moment, research on the use of radiative transfer models focuses mainly on two problems [13]:

- (i) difficulties due to the fact that generally an analytical solution of the inverse problem does not exist. This makes the inversion very time consuming, if one employs numerical optimization techniques;
- (ii) difficulties due to the generally ill-posed nature of the inversion process, which leads to unstable inversion results because some model parameters (for example LAI and average leaf inclination angle) counterbalance each other.

For the first problem it was proposed to use either artificial neural nets (ANNs) [14], [15], [16], [12], or look-up-tables (LUT) [17], [18]. This means that the radiative transfer model is only used in the direct mode to build a (large) synthetic data set. This data set is then used to train the ANN or to build the LUT. Concerning the ill-posed nature of the inversion problem, one has either the possibility to use *a priori* information [18], or to derive

additional information from the remote sensing data itself, for example from the spectral properties of the surrounding pixels [19].

Especially for low coverages (i.e. $LAI \leq 2$) and in spectral regions where leaf and canopy transmittances are high (nIR), one has also to deal with the influence of the underlying soil, which – under these conditions – has a strong influence on canopy reflectance (Fig. 1). To deal with this effect, an effort was undertaken to empirically calibrate a soil reflectance parameterization, and to integrate this soil parameterization into SAILH+PROSPECT canopy reflectance model [20], [21], [9]. With this coupled canopy reflectance model, the assessment of LAI and canopy chlorophyll content from hyperspectral reflectance data was investigated.

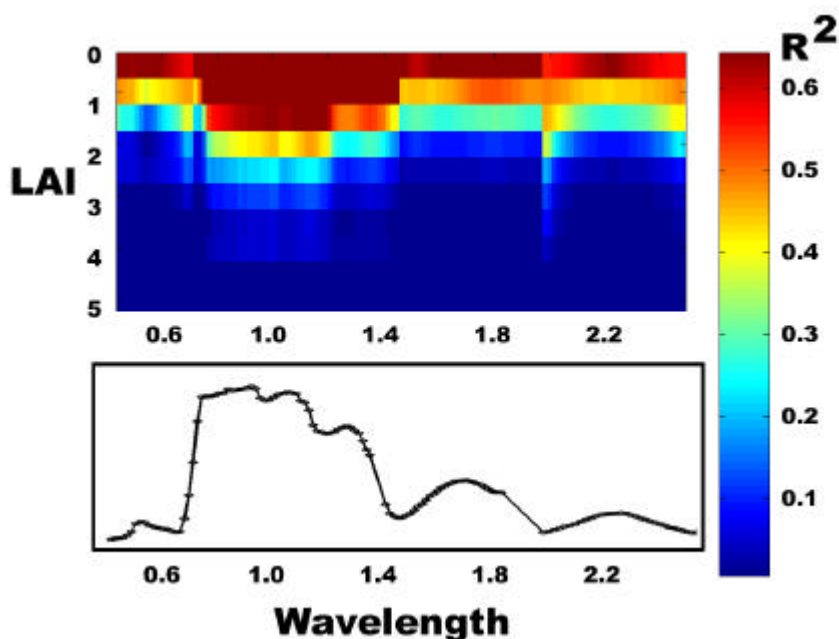


Figure 1. Simulated sensitivity of canopy reflectance to soil brightness as a function of wavelength and canopy coverage (LAI) (top). Sensitivity is expressed by the percentage of variance in the canopy reflectance explained by the soil reflectance (R^2) for the given wavelength and LAI considered. To ease interpretation, a typical vegetation spectrum is also shown (bottom). For the simulation, the extended SAILH+PROSPECT canopy reflectance model was randomly parameterized (parameters shown in Tab. 2). Coefficients of determination (R^2) were calculated between canopy and corresponding soil reflectances.

2 MATERIAL

Four times in the 2000 growing season (Day of Year 119, 130, 162 and 180), four commercial winter wheat fields in the Trier area (“Bitburger Gutland”) were probed (Fig. 2) (for more details see also [6], [7]). Spectroradiometric (Sect 2.1.1) and corresponding leaf area index measurements (LAI) (Sect. 2.2.1) were performed on three randomly chosen sub-plots (0.25 m^2) within each field. From these three measurements, the average LAI values and reflectance spectra were calculated. Average leaf chlorophyll content was assessed from 30 randomly chosen plants collected inside the fields (Sect. 2.2.2). On two occasions, either LAI or chlorophyll measurements were missing; thus, in total, we acquired 14 corresponding spectral and biological measurements that served to validate the canopy reflectance model inversion. Airborne HyMAP data and corresponding final yield measurements (Sect. 2.3) were only used for indirect validation and to demonstrate the general applicability of the approach (HyMAP test site “Feller Hof”) to hyperspectral remote sensing data.

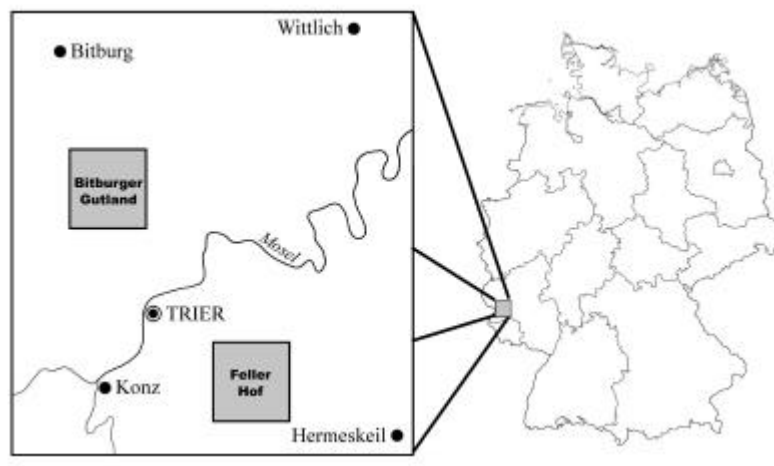


Figure 2. The location of the study region Trier within Germany (right). The validation test site (“Bitburger Gutland”) is situated NW and the HyMAP demonstration site (“Feller Hof”) SE of Trier, respectively.

2.1. Collection of field spectral data

The top of canopy reflectance (1 nm spectral resolution) was measured with an ASD Field Spec Pro spectroradiometer from an height of about 1.5 m during favorable weather conditions around solar noon (integration time: 10 s). ASD readings were normalized to bi-directional reflectances by means of a spectralon reference panel of known reflectivity. For each sub-plot, 5 reflectance readings were taken and averaged. A moving Savitzky-Golay filter (± 5 nm) [22] was applied to reduce sensor noise. Field spectra were resampled to the central wavebands of the HyMAP sensor. The three sub-plot spectra per field were finally averaged to yield the average field reflectance.

2.2. Biological measurements used for model validation

2.2.1 Leaf Area Index (LAI)

On exactly the same positions within the wheat plots where the canopy reflectance was measured, the above-ground plant material was harvested within the 25 x 25 cm sub-plots and brought to the laboratory. There – using a commercial planimeter – one-sided plant surface of the fresh material was determined and used to calculate the leaf area index (LAI; $\text{m}^2 \text{m}^{-2}$).

2.2.2 Canopy chlorophyll content (CAB)

Leaf chlorophyll content was determined using the SPAD-502 instrument [Spectrum Technologies, Inc.]. For each wheat field and measurement date, 30 plants (upper leaves) were randomly selected and probed. SPAD readings were converted into leaf chlorophyll content (Cab; in $\mu\text{g cm}^{-2}$) by means of an empirical calibration function [23]. From the 30 individual leaf chlorophyll measurements, the average was calculated and multiplied by the corresponding LAI (Sect. 2.2.1) to obtain the total canopy chlorophyll content (CAB; in mg m^{-2}).

2.3. Data used for demonstration purposes

To demonstrate the general applicability of the inversion procedure, a HyMAP image was used. The image was acquired in 1999 from an airborne platform and covers the test-site “Feller Hof” (Fig. 2). At the “Feller Hof” test site final yield was measured on 15-08-1999. The HyMAP sensor was flown by DLR on 27-06-1999 and the image was processed at our institute to yield spectral bi-directional reflectances [24]. Processing included parametric geocoding (PARGE software) and atmospheric correction. Since one HyMAP channel was eliminated due to sensor malfunction, the final image had 127 spectral channels and a ground resolution of 5 m.

The intra-field distribution of the final yield (YIELD; in t ha^{-1}) was measured destructively at the end of the 1999 growing season 15-08-1999. Point measurements covering the entire field were made every 5 m within the field ($n_{\text{obs}}=106$). A differential GPS was used to precisely locate the sampling sites. Measured data points were linearly interpolated to space to be directly comparable to the corresponding HyMAP image.

3 METHODS

As shown in (Fig. 1), soil reflectance has a strong influence on canopy reflectance, especially for low coverages. To deal with this effect, a simple soil reflectance parameterization was empirically calibrated, and integrated into SAILH+PROSPECT canopy reflectance model [20], [21], [9]. With this coupled canopy reflectance model, the assessment of LAI and canopy chlorophyll content from hyperspectral reflectance data was investigated. Model inversion was performed using an artificial neural net (ANN) trained on synthetic reflectance spectra generated by the canopy reflectance model (Sect. 3). For validation, an completely independent data set was used, consisting of field reflectance data and corresponding LAI and chlorophyll measurements (Sect. 2). For demonstration purposes, an hyperspectral HyMAP image was also used. The HyMAP derived estimates were empirically related to the final yield of the investigated wheat field.

3.1 Soil parameterization

In an attempt to invert canopy reflectance spectra, it is important to parameterize soil reflectance as realistic as possible, while using only a few parameters. For this purpose, a simple soil parameterization (SOILEMP) was developed. The parameterization considers two main aspects of spectral variability of soils in the study region: (1) changes in the overall brightness, and (2) changes in the shape of the reflectance curve. The overall brightness is mainly influenced by changes in soil moisture content, surface roughness and soil organic matter content. The (minor) changes in the reflectance shape can be related to variations in the inorganic carbon content.

To empirically calibrate the model, a regional soil data base was used [see also [25], [26]]. The data base covers soils from the entire study area and consists of soil spectra and corresponding chemical measurements. From this data base ($n_{\text{obs}}=140$), first the average soil reflectance ($\rho^*_{\text{soil}(\lambda)}$) was calculated. This average reflectance spectrum was then (iteratively) fitted into each measured soil spectra using an (multiplicative) brightness factor (SCALE). In the final step, the remaining reflectance residues (Rsd) were linearly regressed against the inorganic carbon content (C_{inorg}) for each waveband:

$$Rsd_{(I)} = I_{(I)} + S_{(I)} \times C_{\text{inorg}} \quad (1)$$

By doing so, we obtained a simple empirical soil parameterization, which scales and shapes the average soil reflectance spectra according to the overall brightness (SCALE) and the inorganic carbon content (C_{inorg}):

$$\mathbf{r}_{\text{soil}(I)} = \mathbf{r}^*_{\text{soil}(I)} \times \text{SCALE} + Rsd_{(I)} \quad (2)$$

with $I_{(\lambda)}$, $S_{(\lambda)}$ and $\rho^*_{\text{soil}(\lambda)}$ being spectral constants (not shown), and SCALE and C_{inorg} being two wavelength independent parameters.

To evaluate the soil parameterization, it was numerically adjusted to the measured soil spectra (Fig. 3). The overall coefficient of determination (R^2) between measured soil reflectances and fitted values was [0.998] with an RMSE of only [0.001] ($n_{\text{obs}}=17.780$) (Fig. 3 right). Only a few soil samples had spectral properties, that were modeled with R^2 lower than 0.995 (Fig. 3 center). Most wavelengths were modeled with $R^2 > 0.98$ (Fig. 3 left). The slightly lower accuracy for the visible wavelengths is due to the fact, that the actual parameterization oversimplifies reality. For example, it is well known that iron oxide content modifies soil reflectance at shorter wavelengths – a fact currently not included.

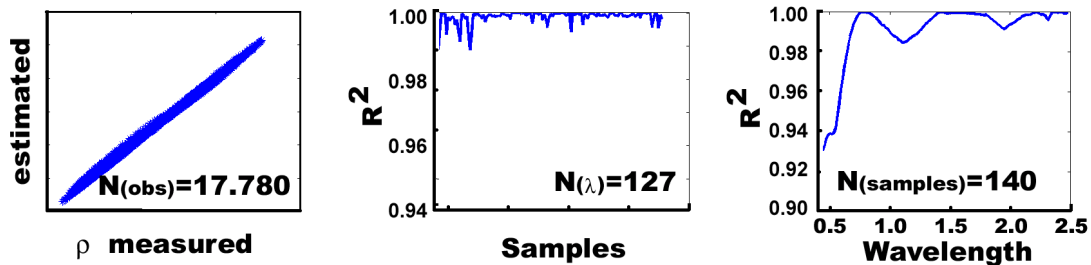


Figure 3. Results of the empirical calibration of the soil reflectance parameterization (Eq. 1 and 2). Measured and adjusted soil reflectance of all soil samples and all wavelengths together (left). R^2 between measured and adjusted soil reflectance for each single soil sample calculated over all HyMAP wavelengths (center). Spectral variation of the coefficient of determination (R^2) between measured and adjusted soil reflectances for all 140 soil samples investigated (right).

3.2 Direct and inverse canopy reflectance modeling

3.2.1 Artificial neural networking

Artificial neural nets (ANN) are able to approximate even very complex (non-linear) relationships [12]. Once trained, ANNs are very fast, even when inverting large data sets. Moreover, they are also able to map several (bio-physical) variables simultaneously and have very low computer storage requirements. Inversion of radiative transfer model using ANNs was shown to be successful on both the leaf and the canopy level [12], [14], [27]. We thus decided to perform canopy reflectance model inversion using an ANN trained on synthetic reflectance spectra generated by the extended SAILH+PROSPECT canopy reflectance model (parameter distributions are shown in Tab. 2). The ANN architecture was set up in a way that 5 parameters of the canopy reflectance model were estimated simultaneously: LAI, canopy chlorophyll content, leaf water content, leaf dry matter content and soil brightness factor. Analysis, however, concentrated on the retrieved LAI and canopy chlorophyll contents.

To avoid network overfitting, the synthetic data set generated by the extended SAILH+PROSPECT model (Sect. 3.2.2) were divided into training data and data used for “early stopping” (i.e. test data). The first subset (2/3 of samples) is used for computing the gradient and updating the network weights and biases. The error on the test data set (1/3 of samples) is monitored during the training process. When the test data error increases for a specified number of iterations, the training is stopped, and the weights and biases at the minimum of the test data error are returned.

Table 1. Main characteristics of the artificial neural net (ANN) employed for canopy reflectance model inversion. Synthetic training spectra were generated by the extended SAILH+PROSPECT canopy reflectance model (see Tab. 2). The ANN was programmed using MATLAB’s Neural Network Toolbox [28]. For further details refer to the text.

ANN architecture	ANN training
Network type	Training patterns
Fully interconnected feedforward network	Synthetic canopy spectra generated by the extended SAILH+PROSPECT reflectance model and compressed into 6 principal components ($n_{\text{obs}}=3.000$) and corresponding model parameters
Number of layers (and corresponding neurons)	Backpropagation training algorithm
3 layers: input layer (6 neurons), hidden layer (2 neurons) and output layer (5 neurons; only LAI and canopy chlorophyll content were used for subsequent analysis)	Levenberg-Marquardt algorithm
Transfer functions of neurons in hidden and output layers	Network performance function
tan-sigmoid (hidden neurons) and linear (output neurons)	Average squared error between network outputs and targets
	Network generalization
	Automatic stop of network training when error on independent test data set increases (“early stopping”)
	Number of training iterations
	50 or less (i.e., when “early stopping” criterion applies)

3.2.2 Generation of training patterns

For ANN training, the extended SAILH+PROSPECT canopy reflectance model was used in the direct mode to simulate 5.000 canopy reflectance spectra in the spectral resolution of the HyMAP sensor. Input parameter combinations were randomly generated. Their statistical distributions were chosen according to the literature, and to represent more or less erectophile wheat canopies (Tab. 2). Only those synthetic reflectance spectra were used further, that fall into the range defined by the reflectance measurements (field and HyMAP spectra) ($n_{\text{obs}}=3.000$) (see Sect. 2). From these synthetic canopy reflectance spectra, the 10 “optimum” wavelengths proposed by [29]

were selected. Three additional wavelengths in the visible part of the spectrum were added (corresponding to the Landsat-TM channels 1 to 3) to cover also those wavebands sensitive to the chlorophyll absorption feature not considered by these authors. The synthetic reflectance data set (13 wavelengths and 3.000 reflectance spectra) was then compressed into the first 6 principle components, covering more than 99.6 % of the total spectral variance. Only these principle components were further used during network training and model inversion.

Table 2. Random parameter sets applied for reflectance modeling of erectophile winter wheat canopies using SAILH+PROSPECT canopy reflectance model, extended by the empirically calibrated soil reflectance parameterization (nadir view; $\theta_z=45^\circ$; $n_{\text{obs}}=5.000$). The parameter sets were randomly generated according to the indicated *distributions* and *ranges*. ⁽¹⁾In cases where *distribution* is *normal*, *range* indicates mean \pm std. ⁽²⁾Cm is drawn such that relative water content is 0.8 ± 0.02 .

<i>model parameter</i>	<i>abbreviation</i>	<i>units</i>	<i>distribution</i>	<i>range</i> ⁽¹⁾
canopy parameter (SAILH)				
Leaf Area Index	LAI	m ² m ⁻²	uniform	0-10
Average Leaf Angle	ALA	° (degree)	normal	70 \pm 3
Hot spot parameter	hot	no dimension	normal	0.1 \pm 0.02
leaf parameter (PROSPECT)				
Leaf chlorophyll content	Cab	g cm ⁻²	uniform	10-80
Leaf water content	Cw	cm	uniform	0.004-0.044
Leaf dry matter content ⁽²⁾	Cm	g cm ⁻²	normal	0.0008-0.016
Leaf structure parameter	N	no dimension	normal	2 \pm 0.34
soil parameter (SOILEMP)				
Soil brightness	SCALE	no dimension	normal	1 \pm 0.14
Inorganic carbon content	C _{inorg}	g cm ⁻³	uniform	0-6

4 RESULTS

4.1 SAILH+PROSPECT inversion using field reflectance data

The SAILH+PROSPECT canopy reflectance model allowed a successful retrieval of the two investigated bio-physical canopy attributes from field reflectance data: LAI and canopy chlorophyll content (Fig. 4). Comparing estimates to ground truth data revealed, that 86 % (LAI), respectively, 87 % (CAB) of the total variance was explained. All points fall close to the 1 : 1 line. No saturation effects are visible. The root mean squared error (RMSE) varied between 0.83 (LAI; m² m⁻²) and 0.66 (canopy chlorophyll content; g m⁻²). An analysis of the residues showed no autocorrelation in the errors (not shown).

The results strongly suggest that the regional calibration of the soil reflectance parameterization and the ANN based inversion strategy, are well suited for the retrieval of bio-physical canopy variables from hyperspectral reflectance data..

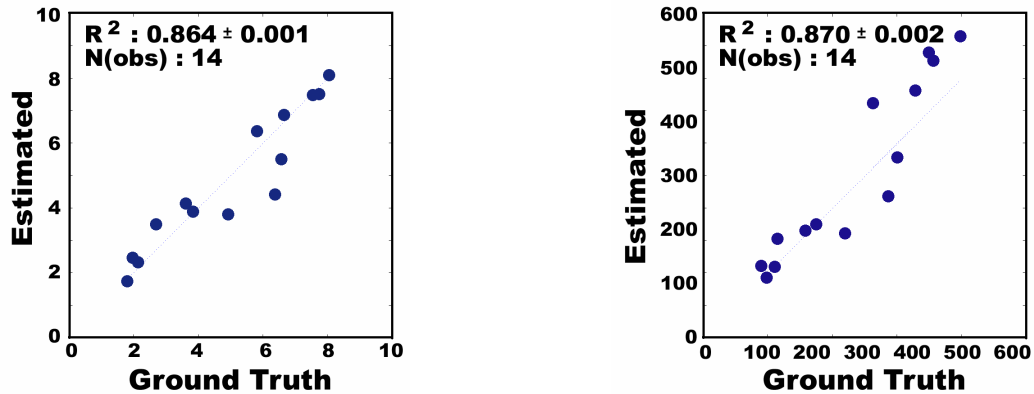


Figure 4. Measured versus retrieved bio-physical canopy variables using hyperspectral field reflectance data and SAILH+PROSPECT canopy reflectance model: LAI (left); canopy chlorophyll content (right). The estimates were obtained using an ANN trained on synthetic canopy reflectance spectra, generated by the extended SAILH+PROSPECT reflectance model. The reference measurements are from a completely independent validation data set (“Bitburger Gutland”). Training and validation was repeated ten times with randomly initialized network weights. The reported coefficients of determination (R^2) are the resulting mean values \pm the corresponding standard deviations.

4.2 SAILH+PROSPECT inversion using HyMAP data

In order to demonstrate the applicability of the inversion approach to airborne data, hyperspectral HyMAP data were inverted to retrieve the bio-physical canopy variables with the same ANN based inversion approach that had previously been used on the field spectra (Sect. 4.1). However, since contemporary reference measurements of LAI and CAB were missing, no direct validation of the retrieved bio-physical variables was possible. Instead, a multi-variate linear regression between the ground measured final yield (YIELD) (dependent variable) and HyMAP derived soil brightness factor (SCALE) and canopy chlorophyll content (CAB) was established. For this regression, 75 % of the reference data were used. The regression revealed a negativ regression coefficient for SCALE and a positiv coefficient for CAB (not shown). This means, final yield in the investigated field was higher in areas with dark soils (e.g., fertile soils) and where LAI and leaf chlorophyll content were high (e.g. high photosynthetic capacity). This indirectly confirms the applicability of the approach to hyperspectral airborne data. The remaining reference data not used for calibration (i.e., 25 % of the total data set) were correlated with the corresponding estimates ($r^2=0.4$) (Fig. 5).

Application of the established multi-variate regression to the HyMAP derived SCALE and CAB values is shown in (Fig. 6 left). The estimated intra-field distribution of the final yield shows more or less the same overall structure than the ground measured yield (Fig. 6 right). However, there are also some strong discrepancies. For example, in the lower right corner of the wheat field, low yield values were measured in the field, because weeds infested this area. Since the sensor (and the retrieval algorithm) do not distinguish between the signal coming from the wheat plants and the signal from the weeds, model inversion (falsly) suggests an area of high final yield.

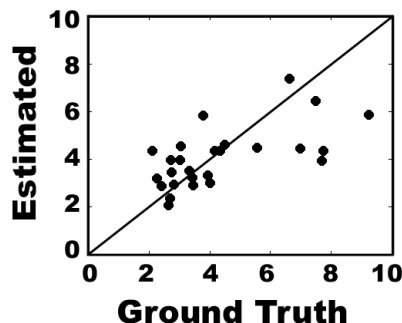


Figure 5. Measured versus estimated final yield ($t\ ha^{-1}$) obtained from a multi-variate regression equation involving HyMAP derived soil brightness factor (SCALE) and canopy chlorophyll content (CAB). The estimates are from an independent data set not used for calibration ($1/4$ of the total data set). Notice the time lag of almost two months between image acquisition 27-06-1999 and ground truth measurements 15-08-1999.

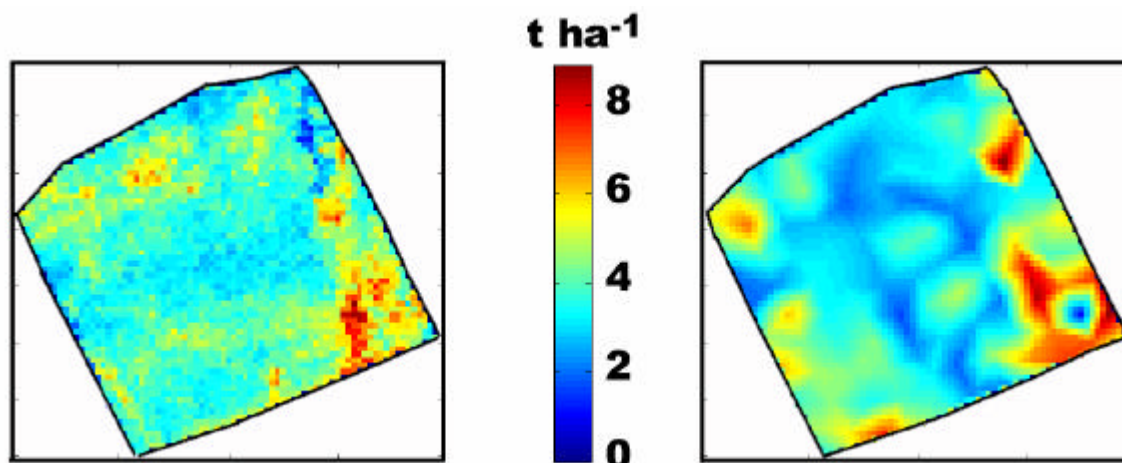


Figure 6. HyMAP derived final yield (left) and corresponding ground measurements (right) (final yield in t ha^{-1}). For the estimates, 75 % of the reference measurements were used to establish a multi-variate regression equation between final yield and HyMAP derived soil brightness factor (SCALE) and canopy chlorophyll content (CAB). This multi-variate regression equation was then applied to the HyMAP derived bio-physical canopy attributes. Notice the time lag of almost two months between image acquisition 27-06-1999 and ground truth measurements 15-08-1999.

CONCLUSIONS

It was demonstrated that the extended SAILH+PROSPECT canopy reflectance model (i.e. coupled with a calibrated soil reflectance parameterization) can be successfully inverted using hyperspectral reflectance data (field and airborne spectra). The ANN based inversion procedure not only proofed exact, but also allowed a very fast inversion of large hyperspectral data cubes.

Direct validation of the field spectra derived bio-physical attributes on completely independent reference measurements gave an R^2 of 0.86 (LAI), respectively, 0.87 (canopy chlorophyll content), with all estimates close to the 1 : 1 line. The root mean squared error (RMSE) varied between 0.83 (LAI; $\text{m}^2 \text{m}^{-2}$) and 0.66 (canopy chlorophyll content; g m^{-2}).

The HyMAP derived bio-physical attributes (soil brightness and canopy chlorophyll content) were successfully related to final yield measurements, acquired almost two month after the image data acquisition. This indirectly confirms the inversion approach

ACKNOWLEDGMENTS

We would like to acknowledge the fundings provided by the German Research Foundation (*SFB 522: Umwelt und Region*) and the University of Trier (*Forschungsfonds and Kapitel 1512*). Thanks to Sebastian Mader, Andreas Marx, Jan Krause and Joachim Hill for valuable help in acquiring the field data and pre-processing the HyMAP data.

REFERENCES

- [1] SCHUELLER, J.K., 1992: A review and integrating analysis of spatially-variable control of crop production. *Fertilizer Research*, 33, pp. 1-34.
- [2] MORAN, S.M., INOUE, Y. AND BARNES, E.M., 1997: Opportunities and limitations for image-based remote sensing in precision crop management. *Remote Sensing of Environment*, 61, pp. 319-346.
- [3] DELÉCOLLE, R., MAAS, S.J., GUÉRIF, M. AND BARET, F., 1992: Remote sensing and crop production models: present trends. *ISPRS Journal of Photogrammetry and Remote Sensing*, 47, pp. 145-161.
- [4] ATZBERGER, C., 1997: Estimates of winter wheat production through remote sensing and crop growth modelling. A case study on the Camargue region. Verlag für Wissenschaft und Forschung, Berlin.
- [5] ATZBERGER, C., GUÉRIF, M. AND DELÉCOLLE, R., 2001: The use of GRAMI crop growth model and SPOT data for biomass estimations in winter wheat. In: Ieroy, M. (ed.): Physical measurements and signatures in remote sensing, pp. 705-711, Balkema Publishers, The Netherlands.

- [6] ATZBERGER, C., JARMER, T., KÖTZ, B., SCHLERF, M. AND WERNER, W., 2003: Spectroradiometric determination of wheat bio-physical variables. Comparison of different empirical-statistical approaches. In: Goossens, A. (ed.): Remote sensing in transition., in press.
- [7] JARMER, T., KÖTZ, B. AND ATZBERGER, C., 2003: Spektrometrische Ableitung biophysikalischer Vegetationsparameter von Weizenbeständen: Vergleichende Untersuchung verschiedener empirisch-statistischer Verfahren. *Photogrammetrie-Fernerkundung-Geoinformatik*, 2003(1), pp. 43-50.
- [8] ATZBERGER, C., 1995: Accuracy of multitemporal LAI estimates in winter wheat using analytical (PROSPECT+SAIL) and semiempirical reflectance models. In: Guyot, G. (ed.): Assessment of remote sensing tools for the estimation of photosynthesis and primary production. Present and future potential, pp. 423-428, Impressions Dumas, France.
- [9] JACQUEMOUD, S., BARET, F., ANDRIEU, B., DANSON, M. AND JAGGARD, K., 1995: Extraction of vegetation biophysical parameters by inversion of the PROSPECT+SAIL Models on Sugar Beet canopy reflectance data. Application to TM and AVIRIS sensors. *Remote Sensing of Environment*, 52, pp. 163-172.
- [10] COMBAL, B., BARET, F., POILVÉ, H. AND POLVERIN, U., 2001: Using multispectral reflectance to retrieve LAI and chlorophyll content of Maize and Soybean. In: Leroy, M. (ed.): Physical measurements and signatures in remote sensing, pp. 499-504, Balkema Publishers, The Netherlands.
- [11] GOEL, N.S., 1987: Models of vegetation canopy reflectance and their use in estimation of biophysical parameters from reflectance data. *Remote Sensing Reviews*, 4, pp. 1-112.
- [12] KIMES, D.S., NELSON, R.F., MANRY, M.T. AND FUNG, A.K., 1998: Attributes of neural networks for extracting continuous vegetation variables from optical and radar measurements, *Int. J. Rem. Sens.*, pp. 2639-2663.
- [13] ATZBERGER, C., 2003: Möglichkeiten und Grenzen der fernkundlichen Bestimmung biophysikalischer Vegetationsparameter mittels physikalisch basierter Reflexionsmodelle. *Photogrammetrie-Fernerkundung-Geoinformatik*, pp. 51-61.
- [14] UDELHOVEN, T., ATZBERGER, C. AND HILL, J., 2000: Retrieving structural and biochemical forest characteristics using artificial neural networks and physically based reflectance models. In: Buchroithner, M. (ed.): A decade of trans-european remote sensing cooperation. pp. 205-211, Balkema Publishers, The Netherlands.
- [15] ABUELGASIM, A. A., GOPAL, S. AND STRAHLER, A.H., 1998: Forward and inverse modelling of canopy directional reflectance using a neural network. *Int. J. Rem. Sens.*, 19, pp. 453-471.
- [16] GONG, P.; WANG, D.X.; LIANG, S., 1999: Inverting a canopy reflectance model using neural network. *Int. J. Rem. Sens.*, 20, pp. 111-122.
- [17] ROWLAND, C.S., DANSON, F.M., NORTH, P.R.J. AND PLUMMER, S.E., 2001: Comparison of neural network and LUT inversion techniques for retrieving forest LAI. In: Leroy, M. (ed.): Physical measurements and signatures in remote sensing, pp. 499-504, Balkema Publishers, The Netherlands.
- [18] COMBAL, B., BARET, F., WEISS, M., TRUBUIL, A., MACÉ, D., PRAGNÈRE, A., MYNENI, R., KNYAZIKHIN, Y. AND WANG, L., 2002: Retrieval of canopy biophysical variables from bidirectional reflectance using prior information to solve the ill-posed inverse problem. *Remote Sensing of Environment*, 84, pp. 1-15.
- [19] ATZBERGER, C., 2002: Object-based retrieval of structural and biochemical canopy characteristics using SAIL+PROSPECT canopy reflectance model: A numerical experiment. In: Sobrino, J.A. (ed.): Recent advances in quantitative remote sensing, pp. 129-138. Publications de la Universitat de València, Spain
- [20] JACQUEMOUD, S., 1993: Inversion of the PROSPECT+SAIL canopy reflectance model from AVIRIS equivalent spectra: Theoretical study. *Remote Sensing of Environment*, 44, pp. 281-292.
- [21] JACQUEMOUD, S., BACOUR, C., POILVÉ, H. AND FRANGI, J.-P., 2000: Comparison of four radiative transfer models to simulate plant canopies reflectance: Direct and inverse mode. *Remote Sensing of Environment*, 74, pp. 471-481.
- [22] SAVITZKY, A. AND GOLAY, M.J.E., 1964: Smoothing and differentiation of data by simplified least square procedure. *Analytical Chemistry*, 36, pp. 1627-1638.
- [23] MARKWELL, J., OSTERMAN, J.C. AND MITCHELL, J.L., 1995: Calibration of Minolta SPAD-502 leaf chlorophyll meter. *Photosynthetic Research*, 46, pp. 467-472.
- [24] HILL, J. AND MEHL, W., 2003: Geo- und radiometrische Aufbereitung multi- und hyperspektraler Daten zur Erzeugung langjähriger kalibrierter Zeitreihen. *Photogrammetrie-Fernerkundung-Geoinformation*, 2003(1), pp. 7-14.
- [25] JARMER, T., UDELHOVEN, T. AND HILL, J., 2003: Möglichkeiten zur Ableitung bodenbezogener Größen aus multi- und hyperspektralen Fernerkundungsdaten. *Photogrammetrie-Fernerkundung-Geoinformation*, 2003(2), pp. 115-123.
- [26] UDELHOVEN, T., EMMERLING, C. AND JARMER, T., 2003: Quantitative analysis of soil chemical properties with diffuse reflectance spectrometry and partial-least-square regression. *Plant and Soil*, accepted for publication.

- [27] SCHLERF, M. ATZBERGER, C., UDELHOVEN, T., JARMER, T., MADER, S., WERNER, W. AND HILL, J., 2003: Spectrometric estimation of leaf pigments in Norway spruce needles using band-depth analysis, partial least square regression and inversion of a conifer leaf model. In: Müller, A. (ed.): this issue.
- [28] THE MATHWORKS, 2000: Neural Network Toolbox for use with MATLAB. The Mathworks, Inc. 3 Apple Hill Drive, MA.
- [29] FOURTY, T. AND BARET, F., 1997: Vegetation water and dry matter contents estimated from top-of-the-atmosphere reflectance data: A simulation study. *Remote Sensing of Environment*, 61, pp. 34-45.